

Chad M. Shafer<sup>1\*</sup>, Joshua G. Hollingsworth<sup>1</sup>, Charles A. Doswell III<sup>2</sup>, Andrew E. Mercer<sup>3</sup>,  
Lance M. Leslie<sup>2,4</sup>, and Michael B. Richman<sup>2,4</sup>

<sup>1</sup>University of South Alabama, Mobile, Alabama

<sup>2</sup>Cooperative Institute for Mesoscale Meteorological Studies, Norman, Oklahoma

<sup>3</sup>Mississippi State University/Northern Gulf Institute, Starkville, Mississippi

<sup>4</sup>University of Oklahoma, Norman, Oklahoma

## 1. INTRODUCTION

Obtaining a comprehensive climatology of severe weather outbreaks is challenging, owing to the rare nature of the events, insufficient observations of severe weather, subjective definitions of what specifically comprises a severe weather outbreak, and nonmeteorological artifacts in the reporting of severe weather. Recent studies by Doswell et al. (2006) and Shafer and Doswell (2010; 2011) have introduced techniques to identify and rank severe weather outbreaks of various types using a linear-weighted multivariate index. In particular, Shafer and Doswell (2011) developed a technique using kernel density estimation (KDE; Brown and Azzalini 1997) to identify severe weather outbreaks of *any type* by associating clusters of severe weather reports with minimum threshold values of the approximated probability density functions (PDFs).

One advantage of the KDE technique is that it objectively identifies *areas* associated with the outbreaks. Although Shafer and Doswell (2011) did not claim that this technique was the sole means of doing so, the identification of regions associated with outbreaks using repeatable methods permits the development of methods to discriminate outbreaks based on relative severity (e.g., Shafer et al. 2010; 2012). In so doing, a climatology of severe weather outbreaks that (1) includes a large sample size, (2) analyzes synoptic and severe weather

diagnostic variables (SWDVs) in the region of interest, and (3) attempts to account for secular trends in the data can be developed. That is the primary purpose of this study.

## 2. DATA AND METHODS

All severe weather reports from 1 January 1960 to 31 December 2010 were considered to rank severe weather outbreaks, as identified by KDE “regions” (see below). North American Regional Reanalysis (NARR; Mesinger et al. 2006) data are used for analysis and model simulations in this study. After minimum threshold report number and density criteria are considered for each KDE region, a set of 4437 cases is obtained (Fig. 1). Outbreak rankings are based on the following severe weather report variables: the total number of reports, tornadoes, severe hail, severe wind, significant tornadoes, significant hail, significant wind, violent tornadoes, killer tornadoes, and long-track tornadoes; total path length of tornadoes; the destruction potential index (DPI; Thompson and Vescio 1998); total number of fatalities; and report density (defined as the total number of reports divided by the total number of grid points in the KDE region). The rankings of the events (based on the N15 index shown in Fig. 1) agree with subjective notions of the relative severity of the events (Shafer and Doswell 2011). For example, events with N15 index scores above zero tend to have multiple significant tornadoes and/or an anomalously large number of significant nontornadic reports, and those with N15 index scores above two tend to be major tornado outbreaks. The Storm Prediction Center (SPC) severe weather database (Schaefer and Edwards 1999) is used to obtain the severe weather reports for the index scores and outbreak rankings.

---

\*Corresponding author address:

Chad M. Shafer  
Department of Earth Sciences  
University of South Alabama  
5871 USA Drive North  
Room 136  
Mobile, AL 36688-0002

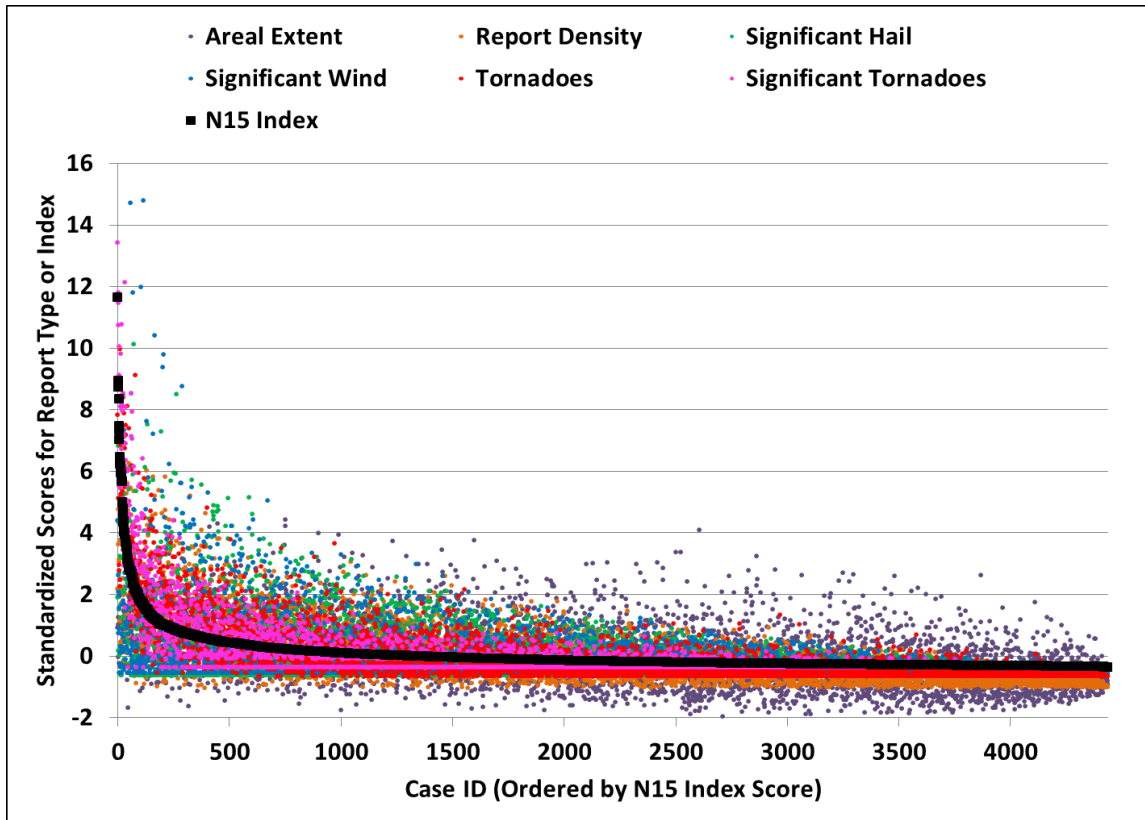


Figure 1: Outbreak ranking index scores (black) and individual report variable scores (detrended and standardized, as detailed in Shafer and Doswell 2011) of 4437 severe weather outbreaks from 1979–2010, as a function of each outbreak’s ranking.

Regions associated with each outbreak are determined via a minimum threshold of the PDF approximated by KDE. The minimum value is chosen subjectively, but is determined based on its ability to (1) distinguish spatially distinct clusters of reports and (2) encompass as many of the reports associated with the event as possible (e.g., Fig. 2). Each grid point in a 300x200 18-km Lambert conformal domain that exceeds the minimum PDF threshold associated with the cluster of reports is considered for that event.

To develop the climatology, several synoptic variables and SWDVs are analyzed for each grid point associated with the outbreak. For a selected variable, the magnitudes are summed, and the average or sum value of the variable is used in the climatology. This so-called areal coverage technique, introduced in Shafer et al. 2012, has been found to be effective in distinguishing the most significant severe

weather outbreaks from less significant events (see Sections 3.3 and 3.4). There are four main tasks of this study. First, as the definition of a major severe weather outbreak is subject to debate, this study attempts to determine which index score thresholds can be distinguished best by the technique. Second, this study analyzes synoptic variables (such as sea-level pressure, geopotential height, wind speed and direction, temperature, dew point, etc.) in addition to SWDVs. Third, analyses of the technique in a forecast setting and comparisons to SPC forecasts are provided. Finally, probabilistic techniques associated with the fields of SWDVs are proposed.

### 3. RESULTS

#### 3.1 Synoptic Variables

Using the map projection described in Section 2 (see Shafer et al. 2010 for a description of the domain, their Fig. 3),

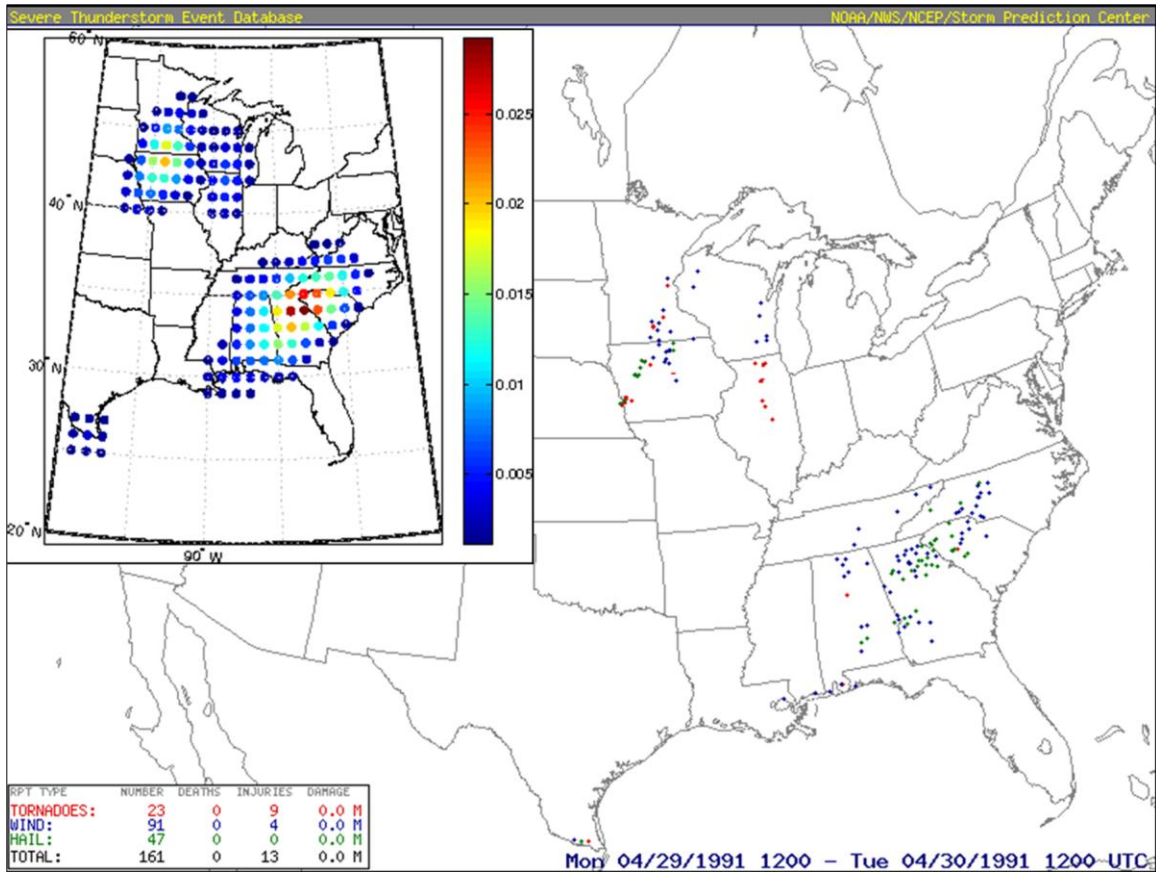


Figure 2: Severe reports from 1200 UTC 29 April 1991 to 1200 UTC 30 April 1991, and the regions associated with the severe weather report clusters (inset), as determined by the KDE technique developed by Shafer and Doswell (2011).

average values of synoptic variables are computed for each event. Outbreaks are separated into four groups for this analysis: those with N15 index scores below zero, between zero and one, between one and two, and at or above two. The most significant outbreaks have a tendency to feature relatively strong winds and low geopotential heights at all levels of the atmosphere, and slightly lower sea-level pressures (Figs. 3 and 4). Additionally, the 500-hPa wind directions tend to be westerly or southwesterly for the most significant events, with few major outbreaks featuring northwesterly flow. This is clearly tied to the times of year in which the events occur (Figs. 3b,d). That is, as events occurring in the summer tend to have average wind speeds considerably less than those in the cool season, northwest-flow events (occurring primarily in the summer) tend not to be significant severe weather outbreaks.

A primary observation is the considerable number of less significant events that also feature similar average magnitudes of synoptic variables. This is an indication of the false alarm problem that has been observed in numerous severe weather discrimination studies (e.g., Rasmussen and Blanchard 1998; Thompson et al. 2003; Shafer et al. 2010), and of pattern recognition techniques in particular (see discussion in Doswell et al. 1993).

### 3.2 Severe Weather Diagnostic Variables

A climatology of SWDVs derived from physical processes associated with severe weather [e.g., storm-relative environmental helicity (SREH; Davies-Jones et al. 1990), convective available potential energy (CAPE), bulk wind shear, the energy-helicity index (EHI; Hart and Korotky 1991), the supercell composite parameter (SCP; Thompson et al. 2003), and the significant

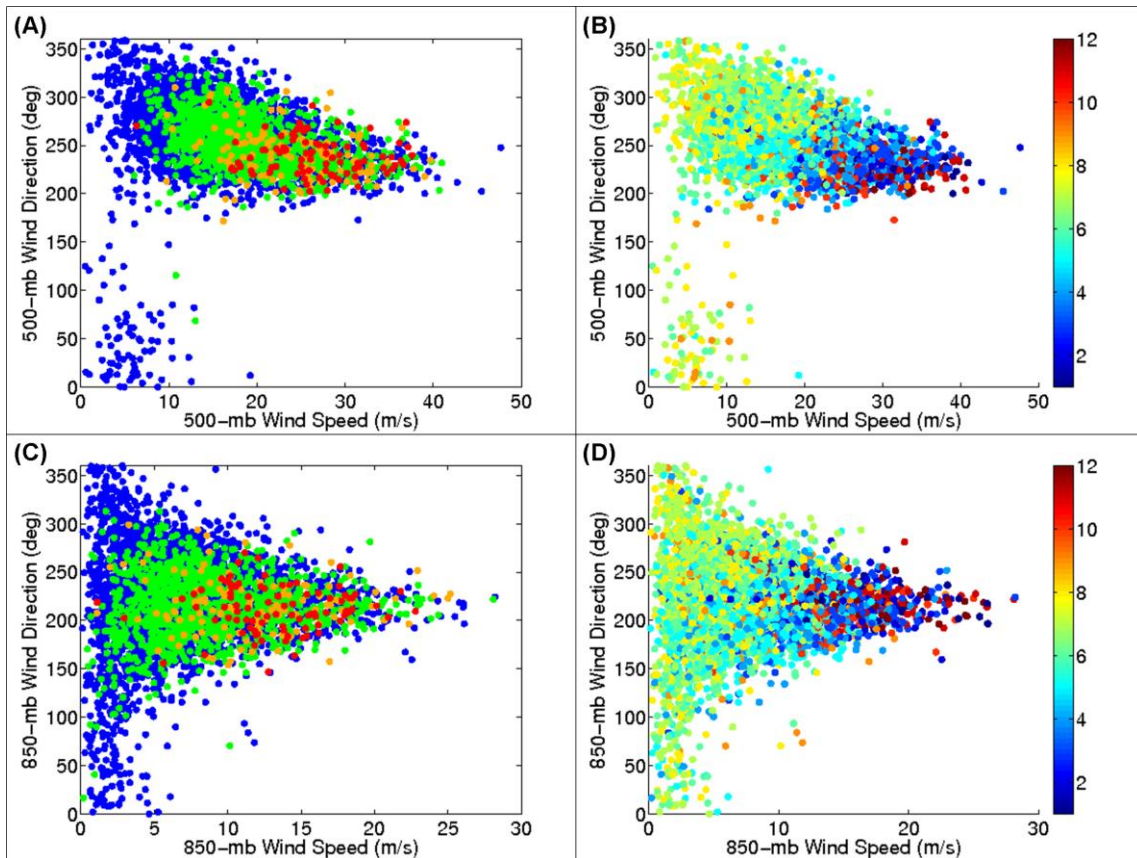


Figure 3: (a) Average values of 500-mb wind speed (x-axis) and 500-mb wind direction (y-axis) for each of the 4437 severe weather outbreaks considered. Red (blue) dots indicate events with N15 index scores above 2 (below 0). Orange (green) dots indicate events with N15 index scores between 1 and 2 (0 and 1). (b) As in (a), except events are indicated by the month number in which they occur. (c) As in (a), except using 850-mb wind speed and direction. (d) As in (b), except using 850-mb wind speed and direction.

tornado parameter (STP; Thompson et al. 2003)] also is conducted for the same 4437 events (e.g., Fig. 5). Using the sums of the diagnostic variables, there is evidence that a subset of the most significant events become separated from (i.e., have higher magnitudes than) the less significant events. This is observed to some degree by the synoptic variables (not shown); however, the utility of SWDVs clearly is suggested here. That is, the most significant outbreaks tend to have higher magnitudes of SWDVs and/or a larger area over which the values are favorable for significant severe weather. This is also in agreement with several past studies discriminating storm type or severe weather type (e.g., Stensrud et al. 1997; Hamill et al. 2005; Shafer et al. 2009).

Clearly, the most significant severe weather outbreaks have a strong tendency to occur outside of the summer season. The results in Figs. 3-5 indicate that this tendency is simply because the conditions favorable for significant severe weather are observed less frequently during the summer. For example, the relatively low number of cases of major tornado outbreaks featuring northwest flow is not because there is northwesterly flow (see Figs. 3 and 6). Rather, the tendency for these events to feature relatively weak winds and shear compared to cool season events with zonal or southwesterly midlevel flow is the reason for the rarity of major outbreaks with northwesterly flow.

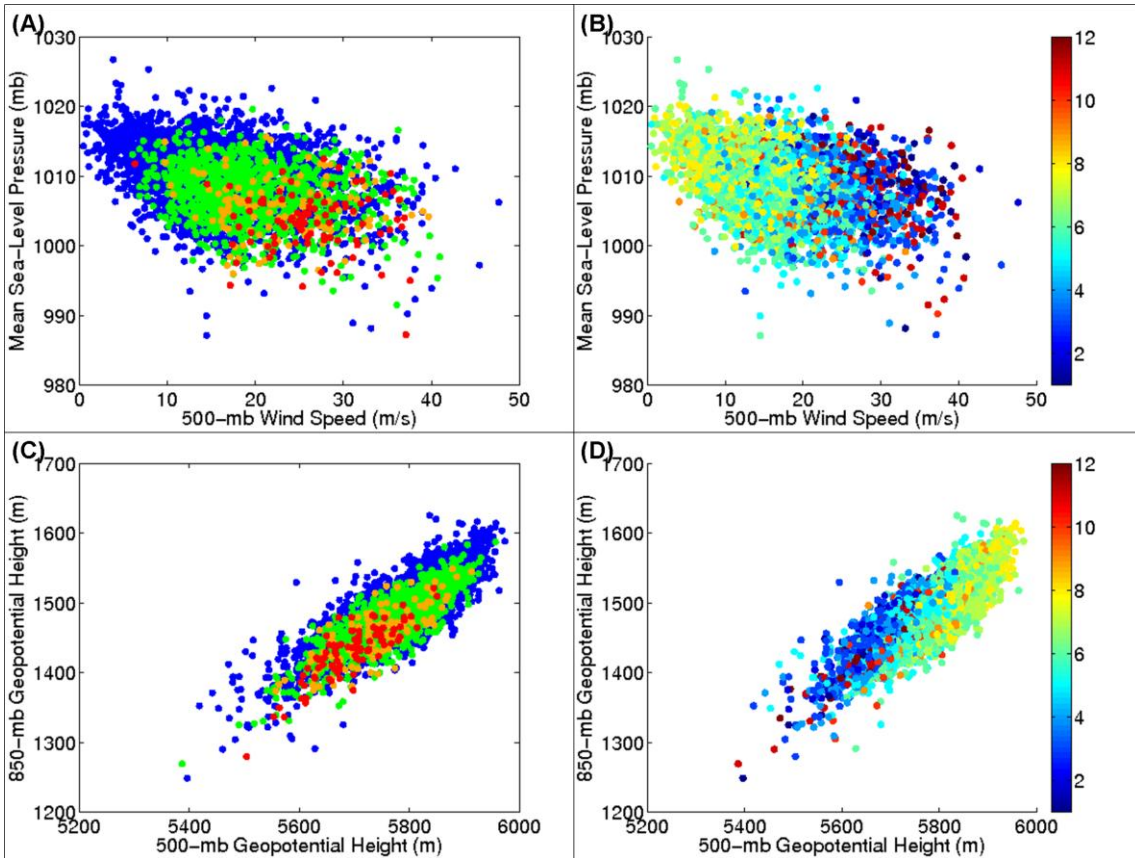


Figure 4: As in Fig. 3, using 500-mb wind speed and mean sea-level pressure [(a) and (b)] and 500-mb and 850-mb geopotential heights [(c) and (d)].

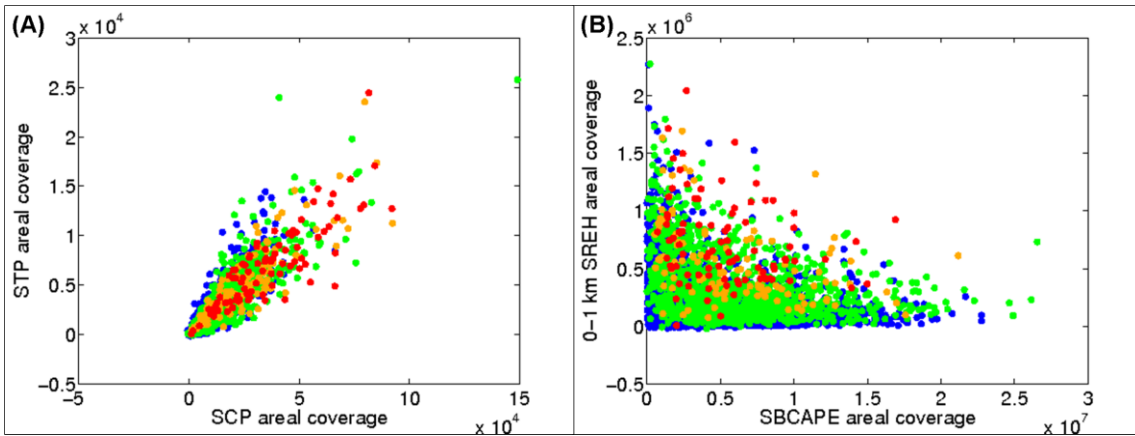
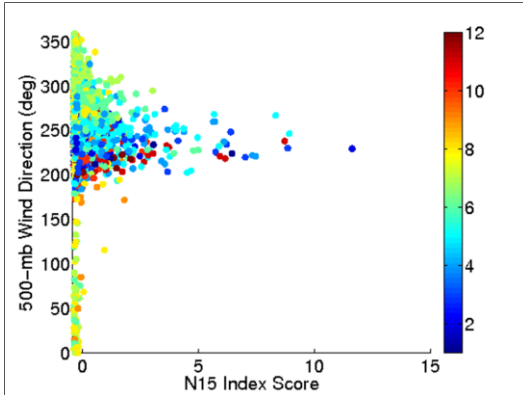


Figure 5: As in Fig. 3a, using the sum values of SCP and STP (a) and surface-based CAPE (SBCAPE) and 0-1 km SREH (b).

### 3.3 Outbreak Discrimination

To determine the utility of areal coverage as a means of discriminating the most significant severe weather outbreaks from less significant events, a value of areal

coverage is selected and tested for incremented values of the N15 index, to determine the index score in which the areal coverage value exhibits the highest skill. Alternatively, one could select a threshold N15 index score to classify events as major



**Figure 6:** N15 index scores (x-axis) and 500-mb wind direction (y-axis) for all 4437 events considered. Month numbers are indicated by the color of the dots.

and minor outbreaks, and determine the value of areal coverage in which the highest skill is exhibited. Combined, both techniques are used to find optimal values of areal coverage that result in the highest skill for any N15 index threshold. Additionally, bootstraps (Efron and Tibshirani 1993) of the skill scores provide some insight regarding the uncertainty of the statistics (95% confidence intervals).

Several SWDVs exhibit considerable skill in distinguishing major and minor severe weather outbreaks (e.g., Figs. 7 and 8). In general, the skill is maximized between N15 index scores of 0 and 1, in which events typically feature multiple significant tornadoes and/or an anomalously large number of significant nontornadic reports. As Section 3.4 suggests, this is consistent with SPC convective outlooks of moderate or high risks of severe weather.

The most skillful SWDVs include SCP, STP, 0-1 km EHI, and 0-3 km EHI – all of which show statistically similar results. These variables all have areal coverage correlations above 0.9, which explains why there is little apparent preference for one variable over the others (for this particular technique). There does appear to be statistically superior skill of EHI versus the product of CAPE and bulk shear (not shown), however, for purposes of outbreak discrimination.

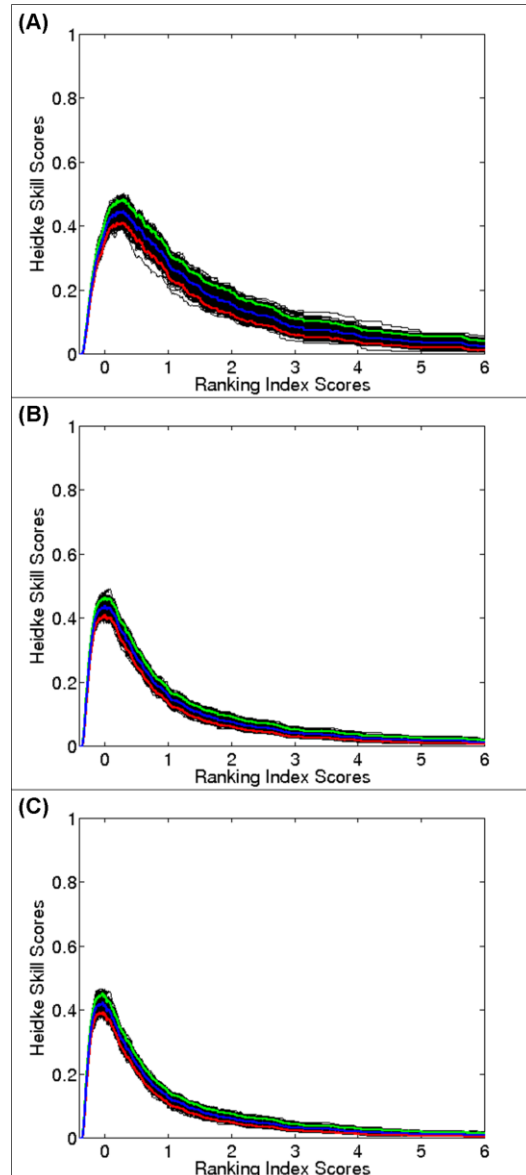


**Figure 7:** Bootstrapped Heidke skill scores of the sum values of areal coverage, using threshold values of (a) 15,000 for SCP, (b) 1500 for STP, and (c) 1500 for 0-1 km EHI, for incremented thresholds of the N15 index score (x-axis). The median value is shown in blue, the 2.5% value is shown in red, and the 97.5% value is shown in green.

### 3.4 WRF simulations

Additionally, the areal coverage technique is tested using model simulations in an attempt to determine the method's potential utility in a forecast setting. The Weather Research and Forecasting model

Table 1: WRF model physical parameterization schemes selected for this study.

Physical Property	Parameterization Scheme
Microphysics	WRF Double-Moment 6-class (WDM6; Lim and Hong 2010)
PBL	Yonsei University scheme (Hong et al. 2006)
Surface	MM5 (from Paulson 1970; Dyer and Hicks 1970; Webb 1970)
Convection	Kain-Fritsch (Kain 2004)
Longwave Radiation	Rapid Radiation Transfer Model (RRTM; Mlawer et al. 1997)
Shortwave Radiation	MM5 (Dudhia 1989)
Land-Surface Model	5-layer thermal diffusion (MM5)

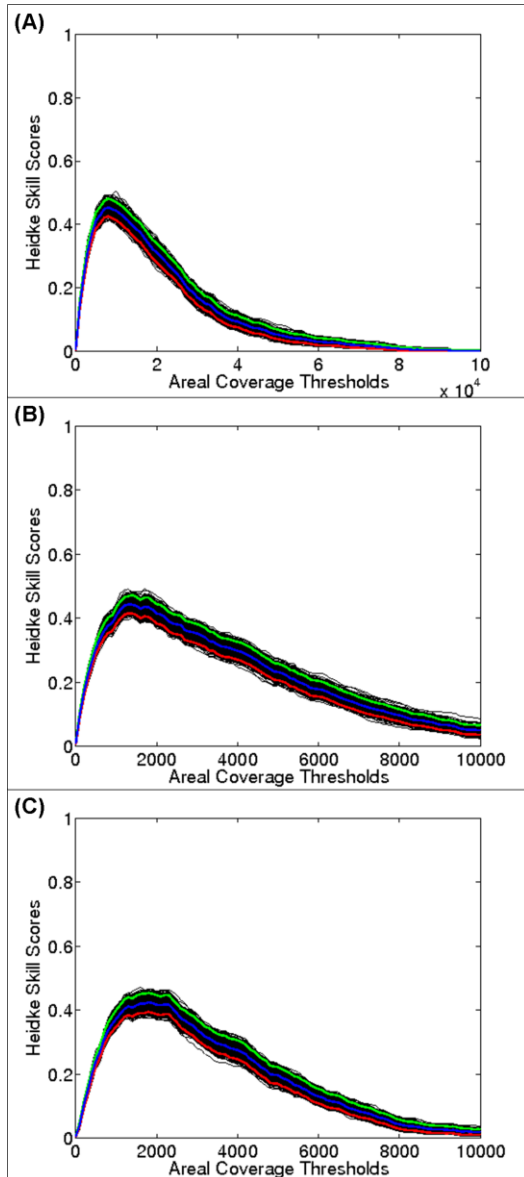


Figure 8: As in Fig. 7, except the N15 index is held at zero, and areal coverage values of (a) SCP, (b) STP, and (c) 0-1 km EHI are incremented (x-axis).

(WRF; Skamarock et al. 2008) is used to complete 970 model simulations for severe weather outbreaks occurring from 2003–2010. Each simulation is initialized at 0000 UTC on the nominal date of the outbreak, and the simulated fields at the valid times of the outbreaks (determined to be the time of the most recently available NARR analysis before the median time of the reports for a given event) are used to compute areal coverage. For the purposes of this study, it is assumed the region associated with the outbreak is known *a priori*, though tests are underway to incorporate techniques that determine a “simulated region” associated with the forecast outbreak. The simulations are initialized with NARR data and bilinearly interpolated to the 300x200 18-km horizontal grid used for analysis in the above sections. The model physics used for these simulations are provided in Table 1.

The skill scores computed for these simulations are compared directly to SPC convective outlooks. Moderate-risk or high-risk outlooks are assumed to be forecasts of major severe weather outbreaks, with slight-risk or lower outlooks assumed to be forecasts of null events (minor outbreaks). Inclusion of this comparison provides a reasonable means of assessing the areal coverage technique as a viable means of forecasting the significance of severe weather outbreaks.

Heidke skill scores of the 970 simulations are similar to the results of the 4437 events (cf. Figs. 7 and 9). The 95% confidence intervals are considerably larger for the 970 simulations, owing to the smaller sample size. As with the 4437 analyses, there is substantial overlap of the confidence intervals among the SWDVs tested,

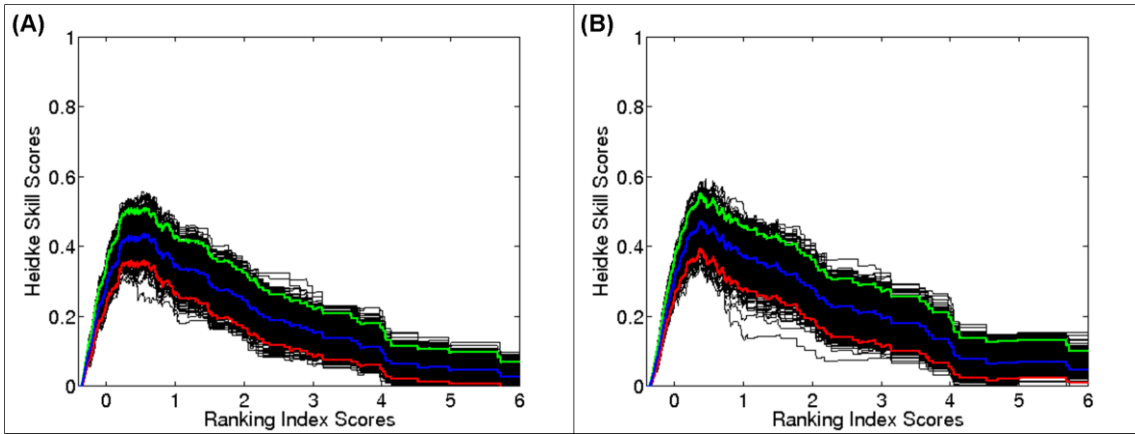


Figure 9: (a) As in Fig. 7, for WRF model simulations of 970 cases from 2003–2010. (b) As in (a), using STP and an areal coverage threshold of 1500.

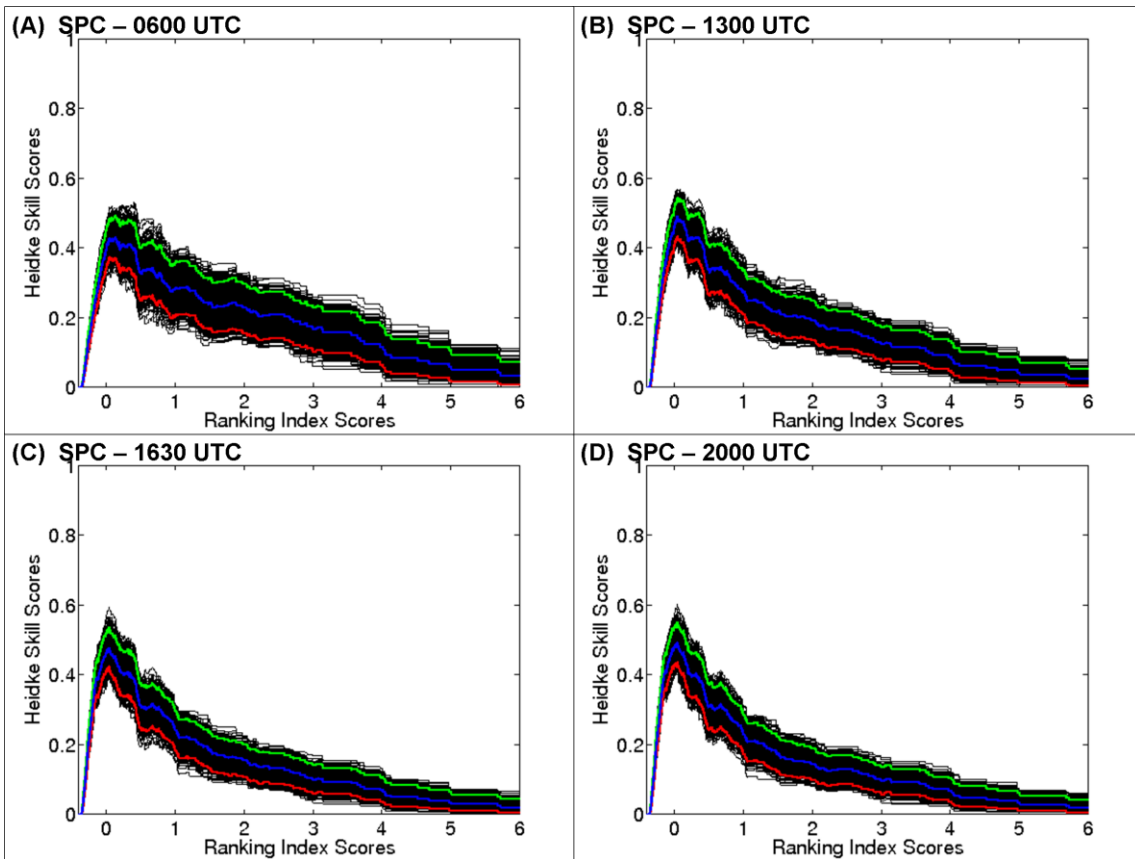


Figure 10: As in Fig. 9, for SPC convective outlooks issued at (a) 0600, (b) 1300, (c) 1630, and (d) 2000 UTC on the nominal dates of the outbreaks. Forecasts of moderate and high risks of severe weather are assumed to be forecasts of major severe weather outbreaks.

indicating a lack of any particular SWDV's superior discriminating capability.

The results in Fig. 9 suggest an apparent increase of the N15 index

threshold for which the maximum Heidke skill scores are observed for the model simulations compared to the analyses (cf. Fig. 7). This is because of two biases observed in the WRF simulations: a

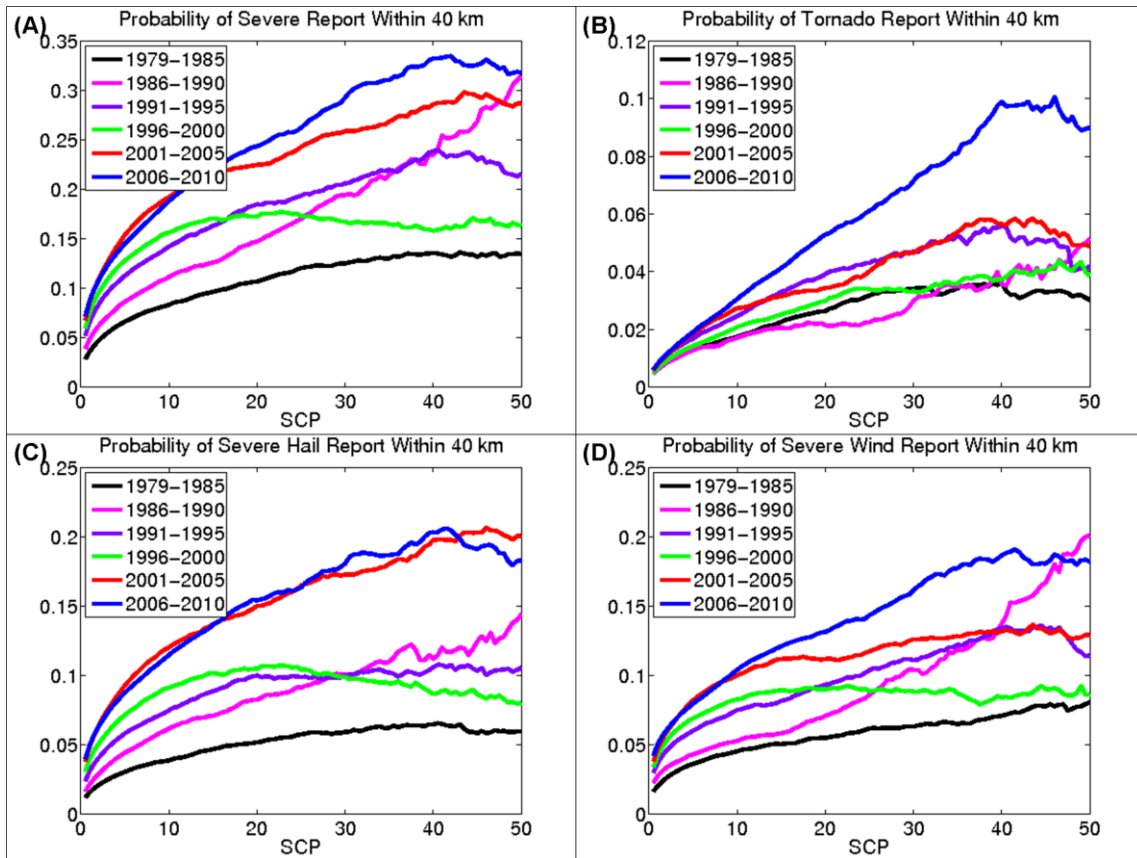


Figure 11: Frequencies (y-axis) of at least one report of (a) severe weather of any type, (b) tornadoes, (c) severe hail, and (d) severe wind occurring within grid points (Lambert-conformal 40-km horizontal grid spacing) equal to or exceeding threshold values of SCP (x-axis). Shown are the frequencies from 1979-1985 (black), 1986-1990 (magenta), 1991-1995 (violet), 1996-2000 (green), 2001-2005 (red), and 2006-2010 (blue).

consistent underforecast of CAPE and a slight underforecast of shear. As both variables are accounted for with SCP (Fig. 9a) and STP (Fig. 9b), these model biases result in a consistent areal coverage negative bias compared to the NARR analyses.

The skill scores found using the areal coverage method are statistically similar to those of SPC convective outlooks issued after the initialization times of the WRF simulations (cf. Figs. 9 and 10). As with the areal coverage technique, Heidke skill scores of the SPC convective outlooks are maximized near N15 index scores of zero. These results suggest that the areal coverage technique can be a useful means of forecasting the severity of outbreaks.

### 3.5 Probabilistic Techniques

Another approach in the development of severe weather outbreak climatologies is the use of probabilistic techniques to associate the magnitudes of SWDVs to the frequency with which severe weather of a certain type or of any type is observed within a predetermined area. For this technique, magnitudes of SWDVs at each grid point in a predetermined domain are obtained. The event frequency is simply the number of grid points that exceed a predetermined threshold value of the SWDV in which at least one severe weather report is observed divided by the total number of grid points in which the SWDV exceeds the threshold magnitude. For example, if 1000 grid points have a SWDV magnitude that exceeds a predetermined threshold, and 300 of those grid points contain at least one severe weather report, the frequency of observed

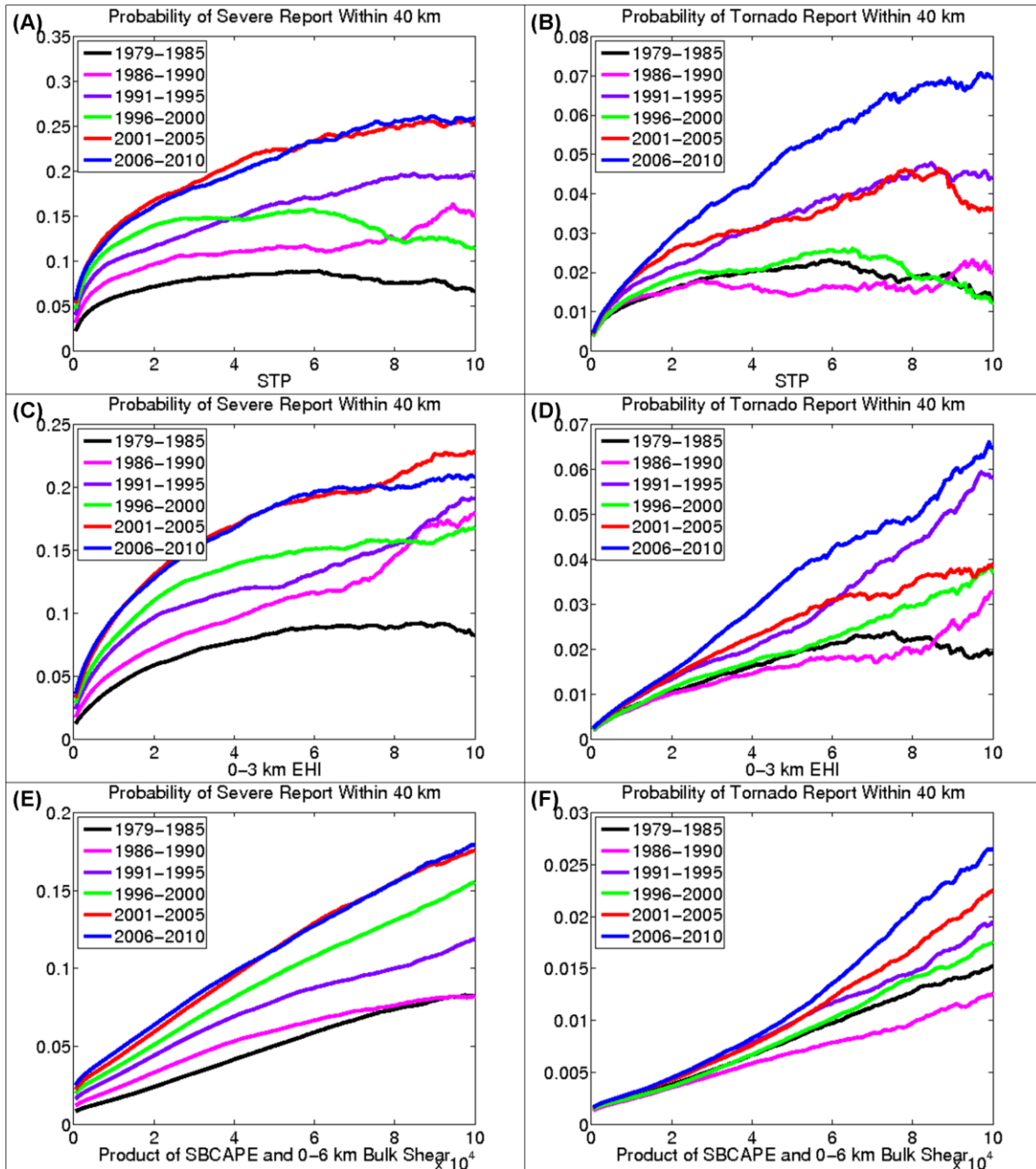


**Figure 12:** (a) As in Fig. 11a, using STP. (b) As in Fig. 11b, using STP. (c) As in (a), using 0-3 km EHI. (d) As in (b), using 0-3 km EHI. (e) As in (a), using the product of SBCAPE and 0-6 km bulk shear. (f) As in (b), using the product of SBCAPE and 0-6 km bulk shear.

severe weather for that SWDV magnitude is 30%.

The fields of SWDVs are obtained for each of the 4437 events considered in previous sections. However, redundant times are removed (i.e., two different events that occur at the same valid time). Only grid points that were included in an outbreak

region at least once in the 4437 events analyzed are considered. Furthermore, all grid points over water are excluded. A Lambert-conformal map projection with 40-km horizontal grid spacing encompassing the conterminous United States is used. This is consistent with previous studies attempting to associate SPC convective outlooks with probabilities of severe weather

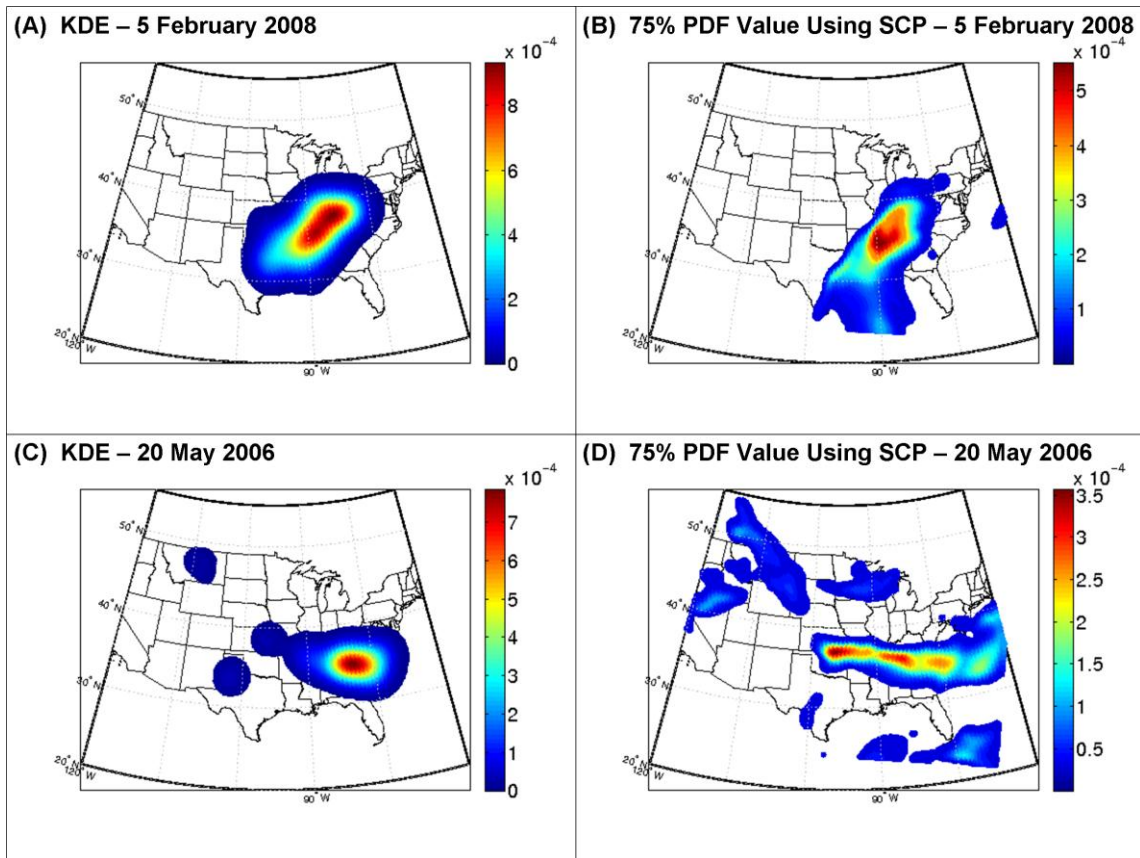


Figure 13: (a) Estimated PDF using KDE (as in Shafer and Doswell 2011) for all reports from 1200 UTC 5 February 2008 to 1200 UTC 6 February 2008. (b) The 75% value of the PDF using SCP magnitudes analyzed at 0000 UTC 6 February 2008, as determined by the 2003–2007 outbreak data. (c) As in (a), for 20 May 2006. (d) As in (b), using training data from 2001–2005 for 20 May 2006.

occurring within a certain distance of a point (e.g., Brooks et al. 1998).

Frequencies of at least one report of severe weather occurring for at least the given magnitude of the selected SWDV generally increase with increased threshold magnitude (e.g., Fig. 11), for any type of severe weather. However, there are obvious secular trends in the data (i.e., the increase in the frequencies at low variable thresholds). Additionally, sample size uncertainties become pronounced at large thresholds (i.e., the variability in the frequencies for subsequent time periods at high SCP magnitudes in Fig. 11). These results demonstrate the need for persistent assessment of associating diagnostic variables to probabilities of severe weather.

The frequencies computed in this technique are *conditional* (i.e., a cluster of severe weather reports must be observed somewhere over the conterminous United States for each time considered). Additionally, the events are defined in 24-h increments (1200 UTC on the nominal date to 1200 UTC the following day – see Shafer and Doswell 2011). However, the large sample size of events considered and the large number of grid points outside of the associated outbreak regions provide a large sample of null grid points to consider. Additional work is planned to determine the frequencies of severe weather in smaller time intervals (down to three hours) for each day in a ten-year period to account for some of these limitations.

This probabilistic approach also can distinguish the relative utility of the SWDVs

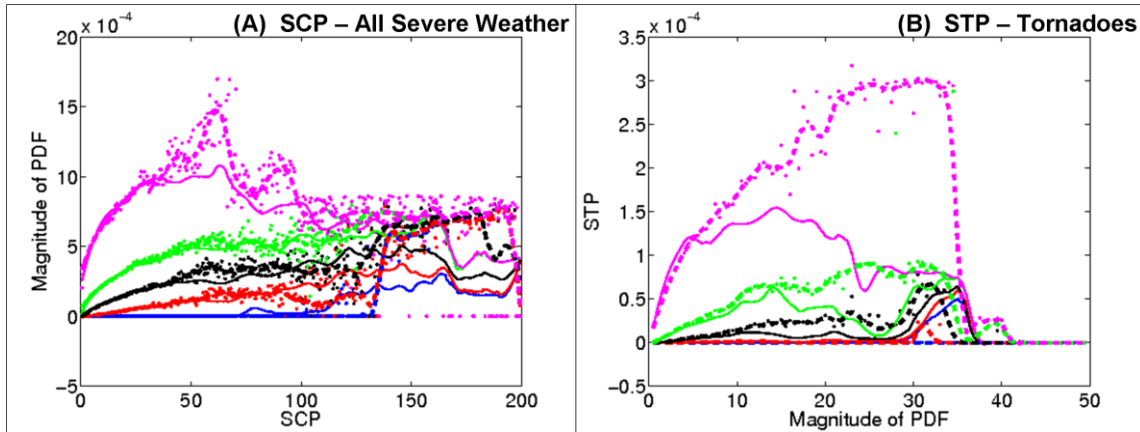


Figure 14: (a) Percentile values (2.5% in blue, 25% in red, 50% in black, 75% in green, and 97.5% in magenta) of the PDFs (y-axis) for all severe weather reports as determined by the magnitudes of SCP (x-axis) at each grid point for all events from 2001–2005 (solid curves using local regression) and from 2006–2010 (points; local regression in dashes). (b) As in (a), using STP and PDFs for tornado reports only.

(see Fig. 12). For example, STP and 0-3 km EHI demonstrate relatively similar frequencies of severe weather of any type or of tornadoes in particular occurring; however, the product of SBCAPE and 0-6 km bulk shear exhibit lower frequencies of severe weather or tornadoes occurring overall.

Alternatively, one could associate the magnitudes of SWDVs with the *density* of observed severe weather reports (as in Fig. 13). To do this, the approximated PDFs (which increase for increased density of the reports) for each of the 4437 events are computed for each grid point in the 18-km Lambert-conformal horizontal grid used in Sections 3.1-3.4 (e.g., Figs. 13a,c). As with the first technique, redundancies associated with events occurring at the same time are excluded.

To develop probabilities of density exceedance, a distribution of PDFs for incremented magnitude ranges of a SWDV (e.g., SCP values from 0.25-0.75, 0.75-1.25, 1.25-1.75, etc.) is obtained. Percentile values of the PDF then are computed for each of these magnitude ranges. These percentile values are frequencies in which the PDFs are at or below the magnitude associated with the percentile selected. For example, the 75<sup>th</sup> percentile value of PDF for the SCP magnitude of 50 for outbreaks considered from 2001–2005 is  $\sim 0.0005$  (Fig.

14a), meaning that 75% (25%) of the grid points with the SCP magnitude of  $50 \pm 0.25$  had PDF magnitudes  $\leq 0.0005$  ( $\geq 0.0005$ ).

The 75<sup>th</sup> percentile values of the PDFs for the 5 February 2008 and 20 May 2006 events (Fig. 13) indicate that there is a strong association between the highest values of SCP (given the higher predicted values of PDF in Figs. 13b,d) and the highest density of reports (given the observed values of PDF in Figs. 13a,c). In this example, the predicted PDF values are based on training the previous five years of events. Using this training technique, the PDF distributions appear to generalize for the magnitudes of the SWDVs in which an adequate sample size is available (Fig. 14). That is, for relatively small magnitudes of the SWDVs (in which a large sample of grid points is available), the PDF distributions between 5-year training and 5-year testing sets are reasonably similar. This is true for all types of severe weather (e.g., Fig. 14a) and individual types of severe weather (e.g., tornadoes in Fig. 14b). As the sample size of grid points available for PDF calculations decreases (i.e., for increasingly large values of the SWDV of interest), the PDF magnitude predicted by the training data does not generalize well (e.g., SCP >50 in Fig. 14a; STP >10 in Fig. 14b). Training data for events spanning a larger number of years suffer from secular trends in the reporting of severe weather (not shown).

The two probabilistic techniques proposed have several limitations. For example, only one analysis time is used to compute the probabilities. The fields of SWDVs valid at the times of the events may not be representative of the environments in which severe weather occurred several hours before or after the analysis time. In future work, the maximum magnitude of the SWDV observed during the 24-h period will be used to compute the probabilities. Furthermore, smaller lengths of time can be used to compute report densities, which may provide a more accurate assessment of probabilities associated with magnitudes of SWDVs. Finally, as alluded to above, events in which the threshold criteria of severe weather report number and density are not considered, and furthermore, days in which no severe weather is observed are not considered. This leads to the computation of *conditional* probabilities.

#### 4. DISCUSSION

The KDE technique introduced by Shafer and Doswell (2011) provides a simple means of obtaining a severe weather outbreak climatology. The area associated with each outbreak, as determined by KDE, is used to evaluate the spatial extent and the average magnitudes of synoptic and SWDVs observed with each event. Subsequently, the so-called areal coverage technique is tested to assess the skill with which the most significant severe weather outbreaks can be distinguished from less significant events. In addition, the observed frequencies of at least one severe weather report occurring within a certain distance of a point in which a threshold magnitude of a SWDV is exceeded, and the percentile values of report densities (represented by PDF values) for a given SWDV magnitude are computed.

The most significant severe weather outbreaks typically feature relatively strong ( $>20 \text{ m s}^{-1}$ ) 500-mb wind speeds in primarily westerly or southwesterly flow and relatively strong ( $>10 \text{ m s}^{-1}$ ) 850-mb wind speeds in primarily southerly, southwesterly, or westerly flow. These events also tend to be associated with relatively low geopotential heights at all levels, and lower than average

sea-level pressure in the region of interest. These results agree with subjective notions of significant severe weather outbreaks, and agree with many previous studies on severe weather discrimination (e.g., Brooks et al. 2003; Hamill et al. 2005).

Additionally, there is a tendency for above average values of most SWDVs (such as bulk shear, SREH, EHI, SCP, STP), which encompass larger areas than in less significant events. This agrees with recent studies on discrimination of outbreak types (Shafer et al. 2009; 2010). The high correlation among many of these variables suggests that there is potential for only limited improvement with the use of multiple variables (see Fig. 5a, e.g.).

The areal coverage of these variables exhibits considerable skill in discriminating major and minor outbreaks of severe weather (maximum Heidke skill scores  $\sim 0.5$ ). Herein, major outbreaks feature multiple significant tornadoes and/or an anomalously large number of significant nontornadic reports. Moreover, the technique appears to be promising in an operational setting, with skill scores of WRF-simulated fields of SWDVs statistically similar to SPC convective outlooks issued after the initial times of the simulations.

Although the probabilistic techniques proposed here have substantial limitations (see the final paragraphs of Section 3.5), the methods show promise in relating the magnitudes of SWDVs to severe weather report frequency and density. As expected, event frequency and report density tend to increase with the magnitude of the SWDV. However, the secular trends in severe weather reporting and the low sample size of grid points with large variable magnitudes suggest large uncertainty. Persistent assessment of these frequencies in the future is necessary for the development of skillful guidance.

The techniques proposed show substantial promise for implementation in an operational setting. Future work includes developing an ensemble framework for the areal coverage technique, computing event frequencies and percentile values of report density at increased temporal resolution,

using multiple SWDVs for calculation of probabilities (including conditional probabilities), and assessing the impacts of model bias on the optimal areal coverage thresholds for distinguishing major and minor outbreaks.

## ACKNOWLEDGMENTS

This work is sponsored by NSF Grant AGS-0831359. We thank the University of Oklahoma Supercomputing Center for Education and Research (OSKER) for providing the computing resources necessary for this project.

## REFERENCES

- Bowman, A. W., and A. Azzalini, 1997: *Applied Smoothing Techniques for Data Analysis: the Kernel Approach Using S-Plus Illustrations*. Oxford University Press, 208 pp.
- Brooks, H. E., M. Kay, and J. A. Hart, 1998: Objective limits on forecasting skill for rare events. *Preprints*, Nineteenth Conf. on Severe Local Storms, Minneapolis, MN, Amer. Meteor. Soc., 552–555.
- , J. W. Lee, and J. P. Craven, 2003: The spatial distributions of severe thunderstorm and tornado environments from global reanalysis data. *Atmos. Res.*, **67–68**, 73–94.
- Bunkers, M. J., 2002: Vertical wind shear associated with left-moving supercells. *Wea. Forecasting*, **17**, 845–855.
- Case, J. L., W. L. Crosson, S. V. Kuman, W. M. Lapenta, and C. D. Peters-Lidard, 2008: Impacts of high-resolution land surface initialization on regional sensible weather forecasts from the WRF model. *J. Hydrometeor.*, **9**, 1249–1266.
- Cheng, W. Y. Y., and W. J. Steenburgh, 2005: Evaluation of surface sensible weather forecasts by the WRF and the Eta models over the western United States. *Wea. Forecasting*, **20**, 812–821.
- Coniglio, M. C., K. L. Elmore, J. S. Kain, S. J. Weiss, M. Xue, and M. L. Weisman, 2010: Evaluation of WRF model output for severe weather forecasting from the 2008 NOAA Hazardous Weather Testbed Spring Experiment. *Wea. Forecasting*, **25**, 408–427.
- Craven, J. P., and H. E. Brooks, 2004: Baseline climatology of sounding derived parameters associated with deep, moist convection. *Nat. Wea. Digest*, **28**, 13–24.
- Davies-Jones, R., D. Burgess, and M. Foster, 1990: Test of helicity as a tornado forecast parameter. *Preprints*, 16<sup>th</sup> Conf. on Severe Local Storms, Kananaskis Park, AB, Canada, Amer. Meteor. Soc., 13–24.
- Doswell, C. A. III, R. H. Johns, and S. J. Weiss, 1993: Tornado forecasting: A review. *The Tornado: Its Structure, Dynamics, Prediction and Hazards*, Geophys. Monogr., Vol. 79, Amer. Geophys. Union, 557–571.
- , R. Edwards, R. L. Thompson, J. A. Hart, and K. C. Crosbie, 2006: A simple and flexible method for ranking severe weather events. *Wea. Forecasting*, **21**, 939–951.
- Dudhia, J., 1989: Numerical study of convection observed during the winter monsoon experiment using a mesoscale two-dimensional model. *J. Atmos. Sci.*, **46**, 3077–3107.
- Dyer, A. J., and B. B. Hicks, 1970: Flux-gradient relationships in the constant flux layer. *Quart. J. Roy. Meteor. Soc.*, **96**, 715–721.
- Efron, B., and R. J. Tibshirani, 1993: *An Introduction to the Bootstrap*. Chapman and Hall/CRC, Boca Raton, Florida. 436 pp.
- Hamill, T. M., R. S. Schneider, H. E. Brooks, G. S. Forbes, H. B. Bluestein, M. Steinberg, D. Meléndez, and R. M. Dole, 2005: The May 2003 extended tornado outbreak. *Bull. Amer. Meteor. Soc.*, **86**, 531–542.
- Hart, J. A., and W. Korotky, 1991: The SHARP workstation v1.50 users guide. NOAA/National Weather Service, 30 pp.

[Available from NWS Eastern Region Headquarters, 630 Johnson Ave., Bohemia, NY 11716.]

- Hong, S.-Y., Y. Noh, and J. Dudhia, 2006: A new vertical diffusion package with an explicit treatment of entrainment processes. *Mon. Wea. Rev.*, **134**, 2318–2341.
- Hu, X.-M., J. W. Nielsen-Gammon, and F. Zhang, 2010: Evaluation of three planetary boundary layer schemes in the WRF model. *J. Appl. Meteor. Clim.*, **49**, 1831–1844.
- Johns, R. H., and C. Doswell III, 1992: Severe local storms forecasting. *Wea. Forecasting*, **7**, 588–612.
- Kain, J. S., 2004: The Kain-Fritsch convective parameterization: An update. *J. Appl. Meteor.*, **43**, 170–181.
- Lim, K.-S. S., and S.-Y. Hong, 2010: Development of an effective double-moment cloud microphysics scheme with prognostic cloud condensation nuclei (CCN) for weather and climate models. *Mon. Wea. Rev.*, **138**, 1587–1612.
- Mercer, A. E., C. M. Shafer, C. A. Doswell III, L. M. Leslie, and M. B. Richman, 2009: Objective classification of tornadic and non-tornadic severe weather outbreaks. *Mon. Wea. Rev.*, **137**, 4355–4368.
- Mesinger F., and Coauthors, 2006: North American regional reanalysis. *Bull. Amer. Meteor. Soc.*, **87**, 343–360.
- Mlawer, E. J., S. J. Taubman, P. D. Brown, M. J. Iacono, and S. A. Clough, 1997: Radiative transfer for inhomogeneous atmosphere: RRTM, a validated correlated-k model for the longwave. *J. Geophys. Res.*, **102** (D14), 16663–16682.
- Paulson, C. A., 1970: The mathematical representation of wind speed and temperature profiles in the unstable atmospheric surface layer. *J. Appl. Meteor.*, **9**, 857–861.
- Rasmussen, E. N., and D. O. Blanchard, 1998: A baseline climatology of sounding-derived supercell and tornado forecast parameters. *Wea. Forecasting*, **13**, 1148–1164.
- Schaefer, J. T., and R. Edwards, 1999: The SPC tornado/severe thunderstorm database. Preprints, *11th Conf. on Applied Climatology*, Dallas, TX, Amer. Meteor. Soc., 603–606.
- Shafer, C. M., and C. A. Doswell III, 2010: A multivariate index for ranking and classifying severe weather outbreaks. *Electronic J. Severe Storms Meteor.*, **5** (1), 1–39.
- , and —, 2011: Using kernel density estimation to identify, rank, and classify severe weather outbreak events, 2011. *Electronic J. Severe Storms Meteor.*, **6** (2), 1–28.
- , —, L. M. Leslie, and M. B. Richman, 2010: On the use of areal coverage of parameters favorable for severe weather to discriminate major outbreaks. *Electronic J. Severe Storms Meteor.*, **5** (7), 1–43.
- , A. E. Mercer, C. A. Doswell III, M. B. Richman, and L. M. Leslie, 2009: Evaluation of WRF forecasts of tornadic and nontornadic outbreaks when initialized with synoptic-scale input. *Mon. Wea. Rev.*, **137**, 1250–1271.
- , —, M. B. Richman, L. M. Leslie, and C. A. Doswell III, 2012: An assessment of areal coverage of severe weather parameters for severe weather diagnosis. *Wea. Forecasting*, **in review**.
- Skamarock, W. C., J. B. Klemp, J. Dudhia, D. O. Gill, D. M. Barker, M. G. Duda, X.-Y. Huang, W. Wang, and J. G. Powers, 2008: A description of the Advanced Research WRF Version 3. *NCAR Tech. Note*, NCAR/TN-475+STR, 113 pp. [Available online at [http://www.mmm.ucar.edu/wrf/users/doc/s/arw\\_v3.pdf](http://www.mmm.ucar.edu/wrf/users/doc/s/arw_v3.pdf).]

- Stensrud, D. J., J. V. Cortinas, and H. E. Brooks, 1997: Discriminating between tornadic and nontornadic thunderstorms using mesoscale model output. *Wea. Forecasting*, **12**, 613–632.
- Thompson, R. L., and M. D. Vescio, 1998: The destruction potential index—A method for comparing tornado days. Preprints, *19th Conf. on Severe Local Storms*, Minneapolis, MN, Amer. Meteor. Soc., 280–282.
- , R. Edwards, J. A. Hart, K. L. Elmore, and P. Markowski, 2003: Close proximity soundings with supercell environments obtained from the Rapid Update Cycle. *Wea. Forecasting*, **18**, 1243–1261.
- Webb, E. K., 1970: Profile relationships: The log-linear range, and extension to strong stability. *Quart. J. Roy. Meteor. Soc.*, **96**, 67–90.